

## Swelling of Poly(DL-lactide) and Poly(lactide-co-glycolide) in Humid Environments

J. S. Sharp,<sup>\*,†</sup> J. A. Forrest,<sup>‡</sup> and R. A. L. Jones<sup>\*,†</sup>

Department of Physics and Astronomy, University of Sheffield, Hounsfield Rd., Sheffield, England S3 7RH, and Department of Physics, University of Waterloo, Waterloo, Ontario, Canada N2L 3G1

Received July 5, 2001; Revised Manuscript Received September 20, 2001

**ABSTRACT:** The water uptake of poly(DL-lactide) (PLA) and its copolymer with glycolic acid (PLGA 50:50) has been studied using a quartz crystal microbalance (QCM). The polymers were swollen in humid atmospheres at 20 °C in order to probe both the kinetics of adsorption and the equilibrium amount of water taken up at low concentrations. The relative humidity of the air was controlled using saturated salt solutions. By equating the chemical potentials of the water vapor and the polymer/water mixture at equilibrium, it was possible to extract the Flory–Huggins interaction parameter  $\chi$  from a simple binary mixing theory. Studies were also performed on the formulations of these materials with a model polypeptide active ingredient. The kinetics of swelling were described using a model based on the Thomas–Windle model of penetrant diffusion in glassy polymers.

### Introduction

The uptake of penetrant in a glassy polymer, where the penetrant consists of a good solvent for the polymer, can be described using the Thomas–Windle theory of case II diffusion.<sup>1</sup> The kinetics of penetrant uptake differ from those of a simple Fickian process because the diffusion coefficient is a strong function of the solvent concentration. Rapid swelling of the polymer causes the buildup of osmotic stresses in the material, and further swelling is prevented until these stresses have been dissipated by viscous flow of the stressed polymer chains. As a result, the solvent concentration in the swollen region of the polymer rapidly reaches the equilibrium value, and a swelling front is produced that propagates through the polymer at uniform velocity. The polymer ahead of the front is glassy, but the material behind it is highly plasticized. This front is responsible for the linear mass uptake kinetics that are characteristic of case II diffusion.

Our aim in this study was to look at a system in which high levels of plasticization were expected and determine not only the equilibrium thermodynamic properties but also to try to describe the kinetics of solvent uptake. The polymers studied are of technological interest as drug delivery vehicles and have been granted approval by the United States Food and Drug Administration for use in the body. These polymers are biodegradable and are composed of materials that can be easily removed from the body. They therefore provide a route for producing a nontoxic implantable drug delivery system. The important solvent in biological systems is water, and it plays an important role in mediating both drug delivery and biodegradation of the polymers. So it is important that an understanding be gained about the interaction of these polymers in an aqueous environment.

The polymers used were poly(DL-lactide) and its copolymer with glycolic acid (poly(lactide-co-glycolide)). They have found much application in the field of drug

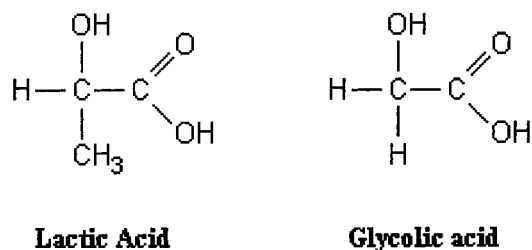


**Figure 1.** Chemical structure of lactic and glycolic acid.

delivery over the past few decades.<sup>2,3</sup> The drugs used can be delivered in a many different ways, but either many authors disperse the drug throughout the polymer matrix in a so-called reservoir device or the polymer is used to coat the drug and form a number of micron sized delivery devices called microcapsules.<sup>4,5</sup> These devices are typically used to deliver polypeptide-based materials directly into the target organ or to dissolve the material in the bloodstream. These types of approaches are used because polypeptides are not readily absorbed in the gastrointestinal tract and so cannot be delivered orally.<sup>2</sup>

The polymers are glassy at body temperature in the unhydrated state but become strongly plasticized as they are hydrated. It is expected that the uptake of water will be influenced by the thermodynamics of the mixing interaction, by the concentration dependence of the mass transport coefficient, and by many-chain relaxation effects in the polymer that arise in response to osmotic stresses. All of these factors are likely to be significantly affected by the presence of an active ingredient.

One of the most attractive properties of these polymers is the fact that they undergo hydrolytic scission of the polyester linkages and break up into natural byproducts which can be easily removed from the body. They are broken down into the components of lactic and glycolic acids and are eventually removed as carbon dioxide and water during the Krebs cycle. The lactide-rich polymers are more hydrophobic than the glycolide-rich ones because of the presence of an extra methyl group on the first carbon (see Figure 1). This has a dramatic effect on the rate of scission of the chains.

<sup>†</sup> University of Sheffield.

<sup>‡</sup> University of Waterloo.

\* Corresponding authors.

PLGA 50:50 has shown biological lifetimes as short as 1–2 months, while PLA can last up to 18 months in the body.<sup>5</sup> This broad range of properties is what has made these polymers ideal candidates for controlled drug release vehicles. Release of any active ingredient from a polymeric device is a complex process that must involve diffusion of water into the polymer matrix, diffusion of the ingredient out of the matrix into the surrounding medium, and time-dependent changes in the polymer properties which are coupled with diffusion processes. Such changes include hydrolytic degradation<sup>7</sup> as well as physical plasticization, and the reciprocal influence of these changes on water uptake and ingredient release mean that the release process cannot be modeled by a straightforward diffusion process.

The purpose of this work is to address these issues by making well-controlled measurements of the equilibrium amounts adsorbed by the materials and of the kinetics of water uptake as a function of the activity of the surrounding water vapor. An attempt is then made to treat these in the context of a simple but robust theoretical framework, based on the Flory–Huggins expression for the free energy of mixing.

The technique used to study the uptake of water in these polymers was the quartz crystal microbalance (QCM). This technique uses a precision piece of AT cut quartz<sup>6</sup> as a resonator, which shears when an ac (sinusoidally varying) field is applied perpendicular to the faces of the crystal. When the shear wavelength is  $2/(2n + 1)$  ( $n = 0, 1, 2, \dots$ ) times the thickness of the crystal a mechanical resonance is set up. This mechanical resonance corresponds to an equivalent resonance in the LCR circuit used to measure the response of the quartz crystal. Changes in the resonant frequency can therefore be probed by monitoring the electrical response of the crystal. When a thin rigid film of material is applied to the surface, it couples to the oscillations of the crystal and changes its resonant frequency. Sauerbrey<sup>8</sup> showed that, for small amounts of material deposited on the crystal surface, the change in frequency caused by the extra mass is directly proportional to the areal density of material deposited on the crystal,  $\Delta m$  (eq 1).

$$\Delta f = - \frac{2f_0^2}{\rho_q v_q} \Delta m \quad (1)$$

where  $f_0$  is the resonant frequency of the unloaded oscillator in its fundamental mode;  $\rho_q$  and  $v_q$  are the density and shear velocity of sound in quartz, respectively.

The use of modern electronics makes it possible to measure frequency changes of  $\pm 0.1$  Hz. So a 10 MHz quartz crystal operating at its fundamental frequency, having a density of  $2650 \text{ kg m}^{-3}$  and a shear sound velocity of  $3340 \text{ ms}^{-1}$ , is capable of detecting a change in the areal density of material deposited on it, equivalent to  $0.5 \text{ ng cm}^{-2}$ . This makes the QCM a very sensitive instrument, and recently it has found much application as a tool for measuring the adsorption of small amounts of material in both gaseous and liquid environments.<sup>9,10</sup>

As well as measuring mass uptake, it is possible to gain information about the energy dissipation in the system. In the Q-Sense technique this is done by fitting the decay envelope of the amplitude of the crystal when it is not being driven. The envelope describes how

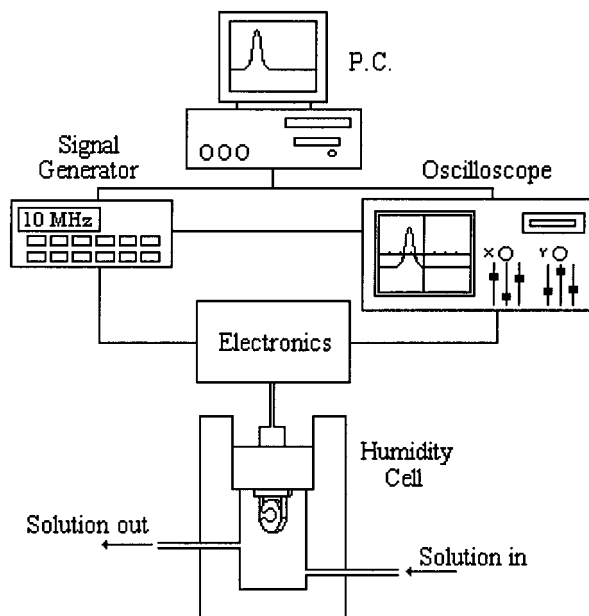


**Figure 2.** Schematic diagram of the Q-Sense quartz crystal microbalance used in this study.

quickly the oscillator is damped out, and from it the dissipation  $D$  can be obtained. This parameter is simply related to the quality factor of the oscillator,  $Q$ , by the relation  $D = 1/Q = E_{\text{dissipated}}/2\pi E_{\text{stored}}$  and can be used to detect changes in the viscoelastic properties of the system being studied.

The idea behind the work presented here is to consider how the properties of the materials studied change as the water content of the polymers is increased. This is done by placing the polymer-coated crystal in an environment where the relative humidity is controlled. The change in resonant frequency caused by the ingress of water is then recorded and related to the mass uptake in the system. A range of water concentrations can be studied by changing the relative humidity of the air surrounding the samples. Then a simple argument based around the Flory–Huggins free energy of mixing can be used to extract the thermodynamic parameter that describes the swelling system.

## Experimental Section

The quartz crystals used in this study were 9 mm diameter 10 MHz AT cut crystals (available from Quartz Pro, Sweden). They consisted of an optically flat piece of quartz with gold electrodes evaporated onto both sides, in a keyhole configuration.

The QCM was obtained from Q-Sense AB, Sweden, and is controlled by a PC (see Figure 2). A signal generator is used to sweep a frequency range in which the resonant frequency is thought to lie, and an oscilloscope is used to look at the voltage response of the crystal as the frequency is changed. When a resonance has been found, the crystal is driven at that frequency and then turned off. The voltage response of the crystal is then monitored as the signal decays. By fitting this decay in real time, to the functional form of eq 2, it is possible to track subsequent changes in the resonant frequency,  $f$ , and the energy dissipation in the system with great accuracy (see Figure 3).

$$V(t) = V_0 \exp(-\pi Dft) \cos(2\pi ft + \delta) \quad (2)$$

where  $t$  is the elapsed time and  $\delta$  is an arbitrary phase factor. The energy dissipated by the system is related to the  $Q$  factor of the oscillator. As mentioned above, the quantity describing

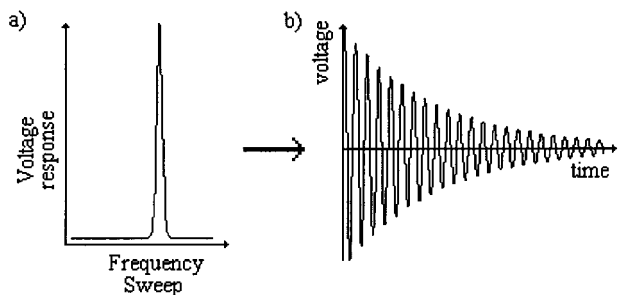


**Figure 3.** Driving frequency is swept over a range enclosing the resonance. The rough position of the resonance is determined, and the crystal is then driven at this frequency and switched off. The decay of the voltage response is fitted to eq 2 using the peak position as a starting point in the Levenberg–Marquardt algorithm.

the envelope of decay of the undriven crystal is the  $D$  parameter. Measurement of this parameter can provide quantitative information about viscous losses in the system.

The equipment used in this study was capable of measuring changes in frequency of  $\pm 0.1$  Hz and changes in dissipation of 1 part in  $10^7$ .

Materials used included 12K and 80K Da poly(DL-lactide) and a 10K Da PLGA 50:50 as well as some 10K Da formulations of the polymers with a model polypeptide active ingredient.

Before the polymer was deposited on to the crystals, the resonant frequency was determined. Films of the polymers were made by dissolving them in chloroform and spin-coating the resulting solutions on to both sides of the crystals. The films were annealed at  $60^\circ\text{C}$ , and the resonant frequency was monitored until constant, to make sure that any solvent present in the films had been removed. The new resonant frequency of the polymer-coated crystal was recorded, and the change in frequency caused by adding the film,  $\Delta f_{\text{film}}$ , was used to calculate the film thickness. The films were typically  $1\text{--}2\ \mu\text{m}$  thick. They were made sufficiently thin to ensure that the uptake of water could be monitored before any degradation of the polymer could take place. The crystals were placed in a specially constructed humidity cell, which was held at  $20^\circ\text{C}$  and flushed with dry air. The relative humidity of the air was measured and was found to be zero. The response of the polymer-coated crystal was then monitored until there was no change in the resonant frequency, i.e., until any water in the films had been removed.

When the residual water had been removed, saturated salt solutions were injected into the cell to provide a controlled humid environment. The volume of the cell used was kept low ( $2\text{--}3\ \text{cm}^3$ ) to allow rapid equilibration of the air above the saturated salt solutions. The frequency response and dissipation of the polymer coated crystal were monitored throughout the experiment as water was absorbed by the polymer.

## Results and Discussion

### Equilibrium Swelling of PLA and PLGA 50:50.

The equilibrium swelling of polymers in solvent vapor can be described in terms of the equilibrium thermodynamics of polymer/solvent mixtures. Here we adopt a method of analysis originally proposed by Flory (more recently by Chen et al.<sup>11</sup>), which involves equating the chemical potentials of the solvent vapor and the solvent in the mixture.

The difference in chemical potential of the solvent vapor,  $\mu_{\text{vapor}}$ , relative to some reference state can be written in the form

$$\mu_{\text{vapor}} = kT \ln a \quad (3)$$

where  $a$  is the activity of the solvent vapor and is defined as being the ratio of the partial pressure of the

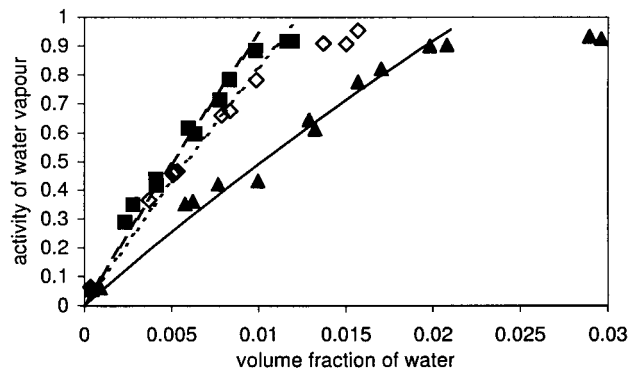


**Figure 4.** Dependence of the equilibrium volume fraction of water on the activity of water vapor in the air surrounding the films. Data are shown along with fits to eq 6. Materials used were (■) 80K Da PLA ( $\chi = 3.63$ ), (◇) 12K Da PLA ( $\chi = 3.50$ ), and (▲) 10K Da PLGA 50:50 ( $\chi = 2.97$ ).

solvent vapor to the vapor pressure of the liquid at a fixed temperature,  $T$ . In the case of water the activity is given by the equation  $a_{\text{water}} = r_h/100$ , where  $r_h$  is the relative humidity of the air.

The chemical potential of the solvent in the polymer/solvent mixture can be derived from the Flory–Huggins theory of mixing<sup>12</sup> to give eq 4,

$$\mu_{\text{pol}} = kT \left( (1 - \phi_w) \left( 1 - \frac{1}{N} \right) + \ln \phi_w + \chi (1 - \phi_w)^2 \right) \quad (4)$$

where  $\phi_w$  is the volume fraction of water in the polymer,  $\chi$  is the Flory–Huggins interaction parameter, and  $N$  is the ratio of the polymer molecular weight to that of the individual monomer units.

Using the Sauerbrey eq 1, the equilibrium volume fraction of water in the polymer films is related to the change in frequency,  $\Delta f_{\text{water}}$ , via the equation

$$\phi_w = \frac{V_w}{V_w + V_p} = \frac{\Delta f_{\text{water}}}{\Delta f_{\text{water}} + \frac{\rho_w}{\rho_p} \Delta f_{\text{film}}} \quad (5)$$

where  $V_w$  and  $V_p$  are the volumes of the water and polymer, respectively;  $\rho_w$  and  $\rho_p$  are the respective densities of the two components. (The densities of the polymers were measured to be  $1254\ \text{kg m}^{-3}$  in the case of PLA and  $1367\ \text{kg m}^{-3}$  for PLGA 50:50.)

Care has to be taken when using the results of the Sauerbrey equation to determine the mass of adsorbed material. Under conditions where the penetration depth of the shear wave is smaller than the system being studied, this expression becomes invalid for describing the amount of water adsorbed by the films. A full description of how to determine this penetration depth and how it affects the applicability of eq 1 to the swelling system described is given at the end of the paper.

By equating (3) and (4), it is possible to describe the equilibrium properties of the mixture in terms of a single parameter,  $\chi$ , that describes the interactions between the polymer and water on a molecular level.

$$\ln a = (1 - \phi_w) \left( 1 - \frac{1}{N} \right) + \ln \phi_w + \chi (1 - \phi_w)^2 \quad (6)$$

A plot of the fits to eq 6 is shown in Figure 4. This plot shows that as the relative humidity of the air surrounding the polymer increases, the amount of water absorbed at equilibrium also increases. It also illustrates

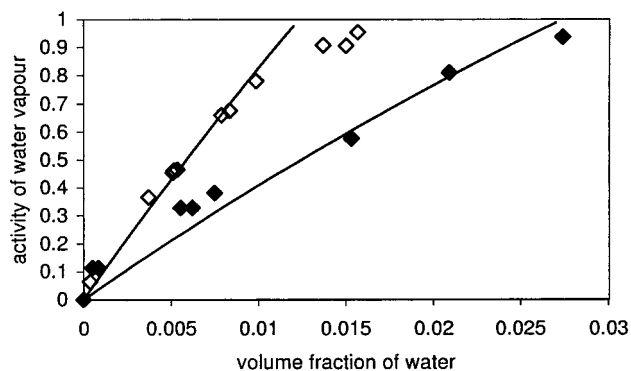


**Figure 5.** Equilibrium uptake of low- $M_w$  PLA and its polypeptide salt. Data are shown for ( $\diamond$ ) 12K Da PLA ( $\chi = 3.50$ ) and ( $\blacklozenge$ ) 10K Da PLA with 15% by mass of polypeptide ( $\chi = 2.80$ ).

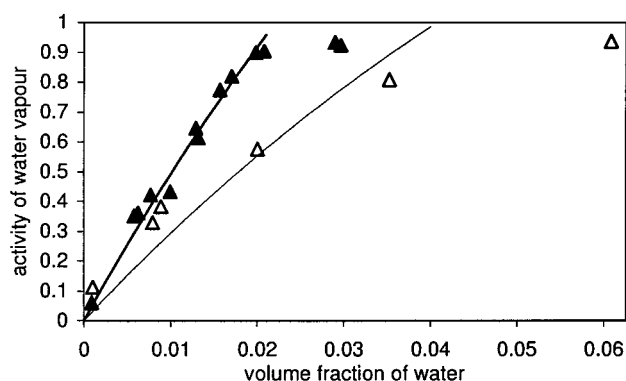


**Figure 6.** Equilibrium uptake of low- $M_w$  PLGA 50:50 and its polypeptide salt. Data are shown for ( $\blacktriangle$ ) 10K Da PLGA 50:50 ( $\chi = 2.97$ ) and ( $\triangle$ ) 10K Da PLGA 50:50 with 15% by mass of polypeptide ( $\chi = 2.46$ ).

that as the molecular weight of the PLA is increased, the mixing interaction becomes less favorable. Figure 4 also shows that the PLGA 50:50 absorbs much more water than the polylactide of similar molecular weight.

Although the curves for the different molecular weights of PLA are very different, the values of the  $\chi$  parameter should be the same. This is because the  $\chi$  parameter represents the energy of interaction of a single monomer with a pure water environment. The residual difference in the observed  $\chi$  parameter for the two molecular weights (3.5 for the 12K Da PLA vs 3.63 for the 80K Da polymer) may be due to the fact that there are more end groups per unit volume in the lower molecular weight material. This effect probably arises because the PLA chains are terminated by carboxylic acid ( $-\text{COOH}$ ) groups. These groups have the effect of making the ends of the polymer chains more hydrophilic than the rest of the macromolecule. If more data sets were available, for a range of molecular weights, then the effective  $\chi$  parameter could be decomposed into two components: one that describes the interaction of the end segments with water,  $\chi_{\text{end}}$ , and a second one that considers the interactions of the rest of the monomers  $\chi_{\text{mon}}$  with the aqueous environment. These individual  $\chi$  parameters would then be weighted by the probabilities of finding each type of monomer to give  $\chi_{\text{eff}} = (2/N)\chi_{\text{end}} + (1 - 2/N)\chi_{\text{mon}}$ . This would allow a more quantitative treatment of the chain end effects.

An extrapolation of the curves in Figure 4 to activities of  $a = 1$  should give the equilibrium behavior of the polymer in bulk water, as this is the point where the vapor pressure is the same as the partial pressure of the water vapor. This means that the chemical potential

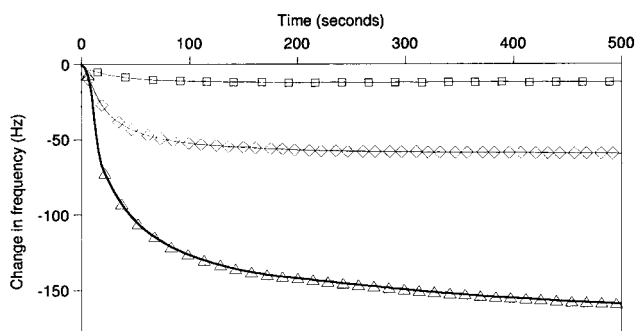


**Figure 7.** Kinetics of swelling in poly(DL-lactide) for polymers hydrated at relative humidities of ( $\square$ ) 6%, ( $\diamond$ ) 37%, and ( $\triangle$ ) 78%.

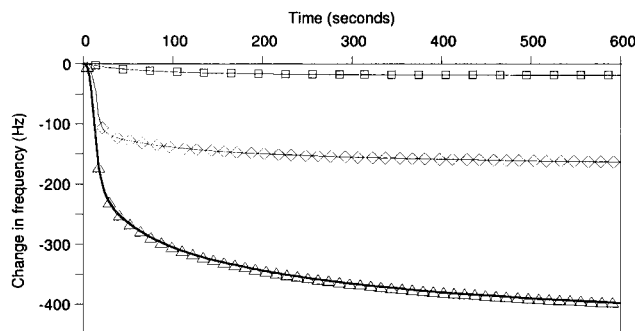


**Figure 8.** Kinetics of swelling in the polypeptide salt of poly(DL-lactide) for relative humidities of ( $\square$ ) 11.3%, ( $\diamond$ ) 38%, and ( $\triangle$ ) 81%.

of the water vapor is identical to that of liquid water. Measurement of the uptake at 100% relative humidity ( $a = 1$ ) proved to be difficult with the QCM, as water droplets condensing on the surface of the polymer gave misleading results. However, bulk water uptake measurements have been performed on PLA using gravimetric methods, and the equilibrium amount of water was found to be 1.4% at 20 °C. This is in reasonable agreement with the swelling data, but there are deviations from the predictions of the simple theory at humidities of 90% and higher. This occurs for all the polymers studied. The amount of water taken up by the polymer is always higher than predicted, and the data appear to show slightly more curvature than is present in the fits. This indicates that the swelling system deviates from the simple Flory–Huggins behavior and cannot be completely described by the model proposed without assigning a concentration dependence to the interaction parameter.

Figures 5 and 6 show the uptake of both PLA and PLGA along with the uptake of their respective polypeptide formulations. The polypeptide is loaded at 15% by mass. The presence of the drug increases the affinity of the polymer for water. This is reflected again in the lower value of the  $\chi$  parameter. For PLA,  $\chi$  is reduced from 3.50 to 2.80 by the addition of the drug, and for PLGA 50:50,  $\chi$  is reduced from 2.97 to 2.46. The measured value of  $\chi$  in these composite systems represents an averaging of the separate interactions between the polymer, drug, and water. More information on the individual interactions would in principle be available for studies in which the drug loading could be varied.

**Kinetics of Swelling.** The kinetics of swelling have similar properties for both the loaded and unloaded systems. Typical plots of the uptake of water are shown in Figures 7 and 8. They show that as the humidity is

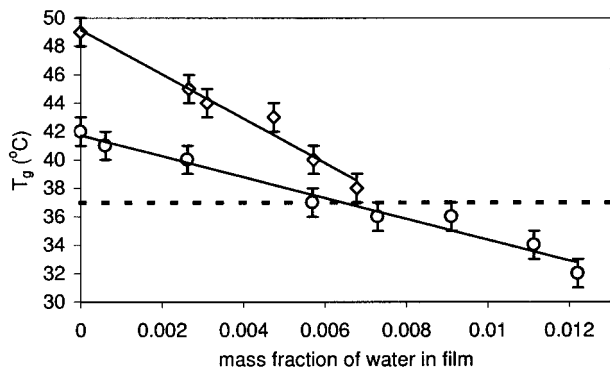


**Figure 9.** Reduction of the  $T_g$  of PLA by the addition of water for samples hydrated above saturated salt solutions. Data are shown for (○) 12K PLA and (◇) 80K PLA.

increased, the initial rate of uptake increases but also that the total equilibration time increases. This latter stage in the kinetic behavior is not expected for mass transport in polymeric materials, because the diffusion coefficient is expected to increase with increasing water content.

The plasticization of PLA by water was investigated by hydrating samples above saturated salt solutions and then using a Perkin-Elmer Pyris II DSC with heating and cooling rates of  $10\text{K min}^{-1}$  to determine the  $T_g$ . Figure 9 shows how the  $T_g$  of the polymer depends on the concentration of the water. It illustrates that over the composition range studied the  $T_g$  becomes suppressed by  $10\text{ }^\circ\text{C}$  in the case of 12K PLA and by  $11\text{ }^\circ\text{C}$  for 80K PLA. The concentration dependence of the diffusion coefficient can be expressed in terms of the WLF shift parameter (eq 7), by incorporating the concentration dependence of the  $T_g$  shown in Figure 9.

$$a_T = \frac{D(T)}{D(T_g)} = \exp\left(-a \frac{T - T_g}{b + T - T_g}\right) \quad (7)$$

The parameters  $a$  and  $b$  are approximately the same in all glass forming systems, with  $a \approx 16$  and  $b \approx 50\text{ K}$ .<sup>13</sup> Using eq 7 for 12K PLA, which has a dry  $T_g$  of  $42\text{ }^\circ\text{C}$ , a reduction in the  $T_g$  of  $10\text{ }^\circ\text{C}$  would cause an increase in the diffusion coefficient by a factor of 2000 at  $20\text{ }^\circ\text{C}$ . This is not what is observed.

Another perhaps more important result of Figure 9 is that at very low mass fractions of water the  $T_g$  is driven below body temperature ( $37\text{ }^\circ\text{C}$ ). This means that physical properties, such as the viscosity and the storage modulus of the polymer, are changing by orders of magnitude when they are placed in biological environments.

The diffusion coefficient of water absorbed from the liquid phase was measured by immersing a  $1.33\text{ mm}$  thick film of 12K PLA in water at  $20\text{ }^\circ\text{C}$ . The sample was removed at regular intervals, dried in a stream of nitrogen gas, and weighed. The mass uptake was fitted to a simple Fickian, concentration-independent diffusion model, and the diffusion coefficient was found to be  $2.63 \times 10^{-11}\text{ m}^2\text{ s}^{-1}$  (see Figure 10). This value is consistent with that of water in similar polymers.<sup>17</sup> In reality, the diffusion coefficient of water in PLA is likely to be highly concentration dependent, and as the polymer is plasticized, it will vary by orders of magnitude. The fitted value therefore represents an average of  $D_c(\phi)$  over the composition range  $0 < \phi < \phi_{\text{eqm}}$ , where  $\phi_{\text{eqm}}$  is the equilibrium volume fraction of water in the polymer. It

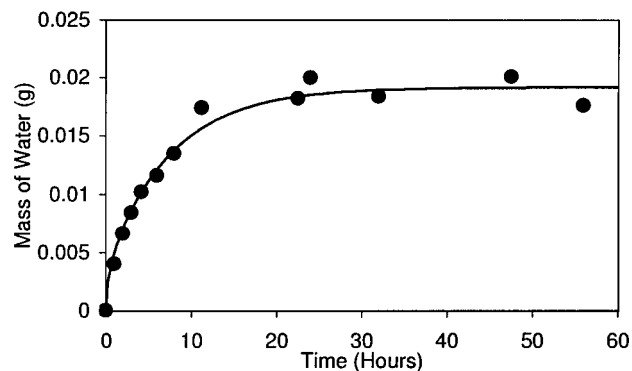


**Figure 10.** Bulk uptake of water in a low- $M_w$  PLA film (thickness  $1.33\text{ mm}$ , mass  $1.3201\text{ g}$ ) is consistent with a Fickian process having a diffusion coefficient of  $2.63 \times 10^{-11}\text{ m}^2\text{ s}^{-1}$ .

is worth stressing at this point that this measurement represents the direct uptake of water from the liquid phase and that the sample used was displaying properties that are characteristic of the bulk polymer.

The kinetics of water uptake obtained in the thin film experiments are much slower than those expected for a bulk system. A diffusion coefficient of  $2.63 \times 10^{-11}\text{ m}^2\text{ s}^{-1}$  implies that the time taken for a  $2\text{ }\mu\text{m}$  film to equilibrate in a pure water environment would be of the order of  $1\text{ s}$ . The films used in the above experiments show equilibration times that are much longer than this (typically hundreds of seconds). Using a simple form of analysis and assuming a purely diffusive process, the mass transport properties of the films can be checked by simply rescaling the diffusion curves according to the relation  $h_1^2/t_1 = h_2^2/t_2$ . Doing this, taking  $h_1$ ,  $t_1$  and  $h_2$ ,  $t_2$  as the thickness and equilibration time of the bulk sample and thin film, respectively, with  $t_1 = 30\text{ h}$ ,  $h_1 = 1.33\text{ mm}$  (from Figure 10), and  $h_2 = 0.002\text{ mm}$ , the equilibration time for the  $2\text{ }\mu\text{m}$  film is calculated to be  $t_2 = 0.24\text{ s}$ . The equilibration time in the films swollen in humid atmospheres was approximately  $300\text{ s}$  for the fastest process (lowest humidity). This is 3 orders of magnitude larger than the value predicted by the simple scaling analysis and confirms that water uptake under these conditions cannot be described by a simple Fickian process.

We have thus established that the uptake of water by  $2\text{ }\mu\text{m}$  films is not governed by the simple diffusive processes that are responsible for water transport in bulk samples. A possible source of this discrepancy might be that the water uptake is somehow limited by transport of the water through the air. This possibility can be eliminated by performing a simple calculation to compare the water transport properties of air with those of the polymer. A measure of the permeability of a material to water can be defined as a product of the diffusion coefficient and the solubility of water in that material. Doing this for air, the calculated solubility (assuming the validity of the ideal gas law for water) is  $0.017\text{ kg m}^{-3}$  and the diffusion coefficient of water vapor in air is  $0.242 \times 10^{-4}\text{ m}^2\text{ s}^{-1}$  at  $20\text{ }^\circ\text{C}$ .<sup>15</sup> This gives a "permeability" of  $4 \times 10^{-7}\text{ kg m}^{-1}\text{ s}^{-1}$  for water in air. This is 3 orders of magnitude larger than the permeability of water in the polymer, calculated from the data obtained for 12K PLA. So the uptake of water by the films is clearly not limited by transport of water vapor through the air.

Confinement effects on the dynamics of thin films are not typically observed for film thicknesses greater than

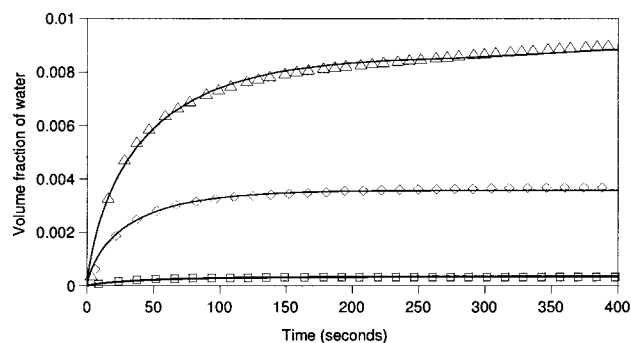


**Figure 11.** Change in volume fraction of water in the films can be accurately determined by solving eq 9. Data are shown, along with the fits, for 12K Da PLA swollen in relative humidities of (□) 6%, (◇) 37%, and (△) 78%.

the average end-to-end distance,  $R_{ee} \approx 2R_g$  of the polymer.<sup>14</sup> The  $2 \mu\text{m}$  films used in this study are much thicker than this limit.

A more likely cause of the discrepancy is that the kinetics of swelling of the polymer by the water, rather than the diffusion of water through the polymer, becomes rate limiting for the short exposures relevant in the thin-film experiments. It is the combination of this osmotic swelling and penetrant diffusion that leads to so-called case II diffusion, as described by the Thomas–Windle model.<sup>1</sup> Here we consider whether the data presented above can be explained by the limit of this model for the case in which the diffusion process is fast compared to swelling, a situation previously considered by Hui et al.<sup>16</sup> The model assumes that the driving force for water uptake is the chemical potential difference between the water vapor and the polymer/water mixture. This chemical potential difference is related to the rate of change of the volume fraction of water,  $\partial\phi/\partial t$ , by a coefficient of proportionality,  $\sigma$ , referred to here as the “swelling resistance” (eq 8).

$$\frac{d\phi}{dt} = \frac{1}{\sigma} \Delta\mu \quad (8)$$

The change in volume fraction,  $\phi$ , with time was obtained by integrating eq 8. For the case when  $\Delta\mu \propto \phi$ , eq 8 can be solved analytically, and the solution obtained is a simple single-exponential uptake profile. However, for the polymer/water system studied  $\Delta\mu = \mu_{\text{vapor}} - \mu_{\text{pol}}$  is given by the more complicated expressions for  $\mu_{\text{vapor}}$  and  $\mu_{\text{pol}}$  obtained from eqs 3 and 4.

$$\frac{d\phi}{dt} = \frac{kT}{\sigma} \left( \ln a - (1 - \phi_w) \left( 1 - \frac{1}{N} \right) - \ln \phi_w - \chi(1 - \phi_w)^2 \right) \quad (9)$$

Equation 9 cannot be solved analytically, and so to obtain the uptake profiles, this expression was solved numerically. The resulting form was then fitted to the kinetic data with only one adjustable parameter, namely the swelling resistance,  $\sigma$ .

Figure 11 shows the change in volume fraction with time for the 12K Da PLA along with the fits to the solution of eq 9. Figure 12 shows how the swelling resistance varies with the equilibrium volume fraction of water in the films. Data are shown for both PLA and PLGA. The kinetics are clearly not those of a fully developed case II process, because of the absence of the characteristic linear form. For thicker films, transport in the polymer should become important, and case II

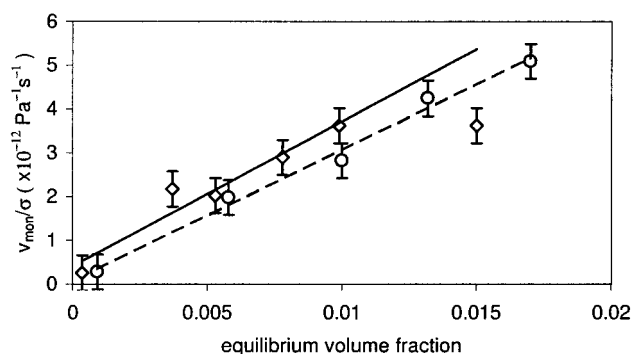


**Figure 12.** Fitted values of the “elongational viscosity”  $\eta = \sigma/v_{\text{mon}}$  varies inversely with the water content. Data are shown for (○) 10K Da PLGA 50:50 and (◇) 12K Da PLA.

behavior may be observed. In this case, the rate-limiting step is no longer the adsorption of material at the polymer/vapor interface but the diffusion of water through the film. The system studied here is behaving more like a small element of polymer which rapidly swells, so that only the osmotic stress relaxation processes are important. In a thicker film made up of many such small elements, only part of the sample is swollen, because the osmotic stresses retard the advancing front, giving rise to the characteristic case II behavior.

The water uptake in the polypeptide formulations of the polymers could not be treated using this approach because the form assumed for the chemical potential does not fit the equilibrium data very well. This means that the form assumed for  $\Delta\mu$  in eq 9 is not correct and does not describe the approach to equilibrium for the swelling system. In principle, an arbitrary form that describes the equilibrium behavior could be used in eq 9. This could then be fitted to the kinetics data for the drug-loaded systems.

The model used by Hui and co-workers<sup>16</sup> assumed that the swelling system was driven by a difference in the osmotic pressure,  $\Delta\Pi$ , across the vapor/polymer interface, such that  $d\phi/dt = \Delta\Pi/\eta$ . The quantity  $\eta$  was described as being an “elongational viscosity” and was used to describe the response of a polymer to the osmotic stresses introduced by the rapid swelling produced by a solvent vapor. The idea is that the polymer is swollen by the solvent, and stresses are introduced which prevent further uptake of material. Only when these stresses have relaxed can further uptake occur. The relevant time scales in this model are set by the “elongational viscosity”.

It is easy to show by a simple substitution that the model of Hui et al. is equivalent to the one presented here, providing that the “elongational viscosity” is assumed to be a weak function of composition over the range studied. It is also possible to write down the relationship between the “swelling resistance”,  $\sigma$ , defined above and the “elongational viscosity” of Hui et al. such that  $\sigma = \eta v_{\text{mon}}$ . Here,  $v_{\text{mon}}$  is the volume of an individual monomer and can be calculated using a simplistic model as being  $v_{\text{mon}} = m_{\text{mon}}/\rho$ . For PLA, the average value of  $v_{\text{mon}}$  was calculated to be  $1 \times 10^{-28} \text{ m}^3$ , and for PLGA 50:50 the calculated value was  $7.8 \times 10^{-29} \text{ m}^3$ . Inserting these values to determine the magnitude of the elongational viscosity yields values of between  $2.8 \times 10^{11}$  and  $2.8 \times 10^{12} \text{ Pa s}$ . The data shown in Figure 12 suggest that the “elongational viscosity” is inversely related to the equilibrium volume fraction over the range of composition studied. PLA does show some

deviation from this form at higher volume fractions, but the PLGA 50:50 data appear to be well described. The observed reduction in this viscosity with increasing water concentration is interpreted as being due to the plasticizing effect of the water.

The viscosities extracted above were compared to those of another polymeric glass. Thomas and Windle<sup>1</sup> measured the viscosity of PMMA using creep tests at temperatures around 20 °C using stresses as high as 10–30 MPa. The values obtained for the viscosity were found to lie between  $10^{14}$  and  $10^{18}$  Pa s. Although measurements of the viscosity of glasses is difficult because of the long relaxation times involved, the measurements of Thomas and Windle serve to give a range of orders of magnitude. At 20 °C, PMMA is 85 °C below its glass transition temperature ( $T_g \approx 105$  °C<sup>17</sup>), but PLA is between 12 and 22 °C below its  $T_g$  at this temperature (Figure 9). Both are glassy, but the PMMA was always at least 63 °C further below its  $T_g$  than the PLA used. This could explain why the viscosities extracted for PLA and PLGA 50:50 are 2 orders of magnitude smaller than those measured for the PMMA system.

The fitted values of  $\sigma$  are the same for both the PLA and PLGA 50:50. This confirms that the contribution due to the thermodynamics is found only in the chemical potential term and that the resistance to swelling originates from how easily the penetrant molecules can enter the polymer matrix. This is probably related to free volume considerations, where molecular weight and the degree of plasticization are important in determining how accessible the matrix is to small molecules.

As the humidity was increased, we found experimentally that the rate of uptake was initially faster, but the total time to reach equilibrium increased. This type of behavior is predicted by the model and is interpreted in the following way. The initial higher rate of uptake observed at higher humidities is caused by the larger driving force for water uptake, which originates from the larger chemical potential difference across the water vapor/polymer interface. The long time processes arise because the initial rapid swelling causes the buildup of osmotic stresses in the films. These stresses are expected to be larger for samples in which the initial rate of sorption is higher and are expected to take longer to completely relax. So for the higher humidities, the osmotic stresses introduced in the early stages of swelling slow down the subsequent rate of water uptake and give rise to longer equilibration times.

**Viscoelastic Energy Dissipation.** The dissipation of energy is an important indicator of the viscoelastic properties of the system. For example, in a glassy polymer the long relaxation times associated with the polymer chains mean that the material cannot deform on the time scales associated with the oscillations of the QCM crystal. In this case the shear wave propagates and experiences little resistance because of the elastic response and low damping in the material. This results in a very slow decay of the oscillations when the QCM crystals are being driven off resonance (Figure 3) and gives rise to a low value for the energy dissipation parameter,  $D$ . A less viscous medium, however, will support a shear because the relaxation times are much shorter. This means that energy will be dissipated and the shear wave attenuated as it tries to propagate through a medium with an increased amount of damping. The result is a more rapid decay of the waveform

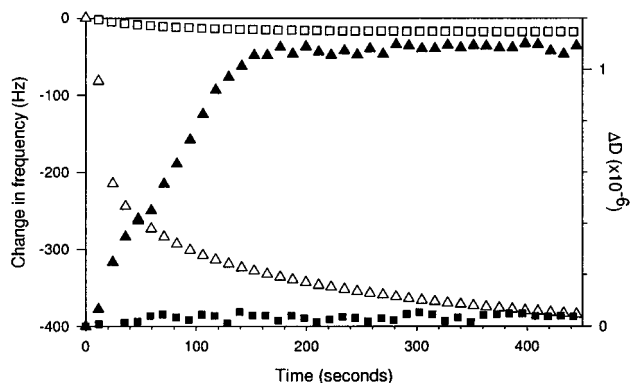


**Figure 13.** Energy dissipation in the films initially mirrors the change in frequency but saturates while the frequency is still changing. Data given are for PLGA 50:50 loaded with 15% polypeptide at relative humidities of 11% (■) and 81% (▲). The hollow symbols show the corresponding frequency changes for comparison.

shown in Figure 3. In the system described here, as more solvent enters the films, we expect that the polymer will become more heavily plasticized. This gives rise to a reduction in the viscosity of the polymer and the corresponding increase observed in the energy dissipation parameter shown in Figure 13.

In the work presented here, the changes in the QCM energy dissipation parameter,  $D$ , were shown to increase between  $10^{-7}$  for a humidity of 11% and  $10^{-6}$  for humidities approaching 80–100%. These changes are small, and in the case of the lower humidities the change in  $D$  is just above the level of noise in the experiment.

During the swelling experiments, the dissipation was found to increase as the water content increased but saturated before the apparent mass uptake (Figure 13). The early saturation of the dissipation in the system was taken as further evidence by Chen et al. of stress relaxation processes which allow more water to enter the films after swelling has apparently ceased. However, this effect could also be attributed to viscous loss mechanisms which are sensitive to changes in composition at small volume fractions of water but which become less sensitive as the volume fraction occupied by water is increased.

The attenuation of the shear wave by a viscous medium is important when considering the validity of the Sauerbrey equation. When considering the validity of eq 1, it is important to have a knowledge of both the penetration depth of the shear wave and the viscosity of the overlayer material.

The position of the glass transition temperature relative to the experimental temperature is also important when determining the validity of eq 1. As mentioned above, a film that is above its  $T_g$  will flow when placed under shear. So the 10 MHz shear wave will be attenuated much more in a film which is capable of dissipating energy via viscous losses than it is in a glassy film which shows a purely elastic response. Rodahl et al.<sup>18</sup> showed that providing the liquid overlayer does not slip on the QCM electrode and that the penetration depth of the shear wave,  $\delta$ , is larger than the thickness of the thin liquid overlayer, then the Sauerbrey relation can be assumed to hold.

The slip condition was generally thought to occur in molecularly thin films, where the monolayers did not couple efficiently to the crystal oscillations. The films

used in this study were microns thick, and no apparent detachment had occurred, so the no-slip condition was assumed.

As mentioned previously, the penetration depth,  $\delta$ , describes how far the shear wave propagates into the surrounding medium (in this case the polymer film). If the film thickness is smaller than the penetration depth, then we can be certain that the whole system is being probed by the shear wave and that any mass changes which occur in the film are detected. Under these circumstances, the Sauerbrey equation is valid. However, if the film thickness is larger than the penetration depth, the shear wave is fully attenuated before it can propagate through the whole film. This means that any mass changes that occur beyond the range of the shear wave are not detected, and the Sauerbrey equation starts to break down. The response of the QCM to a film thicker than the penetration depth therefore becomes equivalent to a system where the crystal is placed in an infinite medium of the overlayer material.

Rodahl et al. showed that  $\delta$  could be determined by means of the simple relation

$$\delta = \left( \frac{2\eta_f}{\omega\rho_f} \right)^{1/2} \quad (10)$$

where  $\eta_f$  and  $\rho_f$  are the viscosity and density of the liquid overlayer and  $\omega$  is the angular frequency of the applied shear wave. The viscosity of fully hydrated PLA measured at 38 °C, at a frequency of 100 rad s<sup>-1</sup> using a Rheometrics Scientific SR5000 stress-controlled rheometer with parallel plate geometry, was found to be 14 803 Pa s. A similar measurement was taken for PLGA 50:50 and was found to be 100 Pa s. These values differ from the viscosity extracted from the swelling kinetics because they represent the shear viscosity of the fully hydrated polymer. The “elongational viscosity” is a different quantity because it represents the response of the glassy polymer to a rapidly advancing solvent front and describes the chain relaxation processes that need to occur before penetrant can enter the glassy material.

Using densities of 1254 and 1367 kg m<sup>-3</sup> for PLA and PLGA 50:50, respectively, we calculated a penetration depth for the shear wave of 613  $\mu$ m for the case of PLA and 48  $\mu$ m for PLGA 50:50 at this frequency. At the much higher frequency of 10 MHz and the lower temperature of 20 °C, these values represent a generous lower bound for the penetration depth of the shear wave into the polymer. This is because the samples measured at 38 °C were much closer to their glass transition temperatures (measured at 10 K min<sup>-1</sup>) than those measured at 20 °C and because the viscosity will be higher at higher frequencies. At 10 MHz, the polymers are expected to have viscosities that are orders of magnitude larger than those given and are expected to show more glass-like behavior. This is because the oscillations produced by the shear wave occur on time scales approaching those associated with the relaxation times of polymer molecules and their individual monomers. As a result, the polymers are unable to flow on the time scale of oscillation, and a more elastic response is observed along with an associated increase in the penetration depth,  $\delta$ . Even though these phenomena need to be considered when calculating the true penetration depth, the calculated lower bounds are sufficient to show that for a 2  $\mu$ m film, swollen in a humid

atmosphere, the Sauerbrey equation is valid. A check was performed by repeating measurements on films of different thickness. The calculated equilibrium volume fractions were the same for a given humidity.

## Conclusion

The quartz crystal microbalance is an extremely sensitive instrument and can be used to probe the uptake of small amounts of water. In the above experiment, the technique was used to quantify the hydrophilicity or hydrophobicity of a system by determining the thermodynamic interaction parameters for interaction between the polymers and water. This was done by using a simple model based around the Flory–Huggins theory of mixing.

The polymers studied were based on poly(DL-lactide) and its copolymer with glycolic acid (PLGA 50:50). Formulations of these polymers with a model polypeptide-based drug were also studied. It was found that for a given molecular weight PLGA 50:50 was the more hydrophilic polymer, having a  $\chi$  value of 2.97 compared to 3.5 for PLA. The model drug used was found to favor the interaction with water, reducing the  $\chi$  parameter from 3.5 to 2.8 in the case of PLA and from 2.97 to 2.46 for the PLGA 50:50.

It was found that the model predicted the equilibrium behavior of the films well at low humidities but at higher humidities (90% and above) failed to give reasonable predictions for the equilibrium volume fraction of water in the polymers. This was attributed to the break down of the assumptions made in constructing the Flory–Huggins theory of mixing. The kinetics of water uptake were also studied, and it was determined that mass transport could not be described by a simple diffusion-limited process. The uptake of water occurred on time scales that are thousands of times larger than expected for such a process. As the humidity of the air was increased, the initial rate of water uptake increased, but the total equilibration time also increased. The kinetics were described by assuming that the driving force for water uptake was the difference in chemical potential between the water vapor and the water/polymer mixture. The model used was found to agree well with the data, and a parameter called the “elongational viscosity” was extracted. This parameter describes the response of a swelling polymer to the osmotic stresses introduced by penetrant uptake.

In conclusion, this paper shows that a simple thermodynamic model can be used to predict the equilibrium behavior of polymers swollen in humid atmospheres. The swelling interaction can then be well described by the use of a single parameter function. The resulting parameter describes the energy of interaction between the polymer and water at a molecular level. The approach to equilibrium can also be described by considering the difference in chemical potential across the vapor/polymer interface as the driving force for water uptake. This again is a one-parameter function, and the parameter describes the response of the system to osmotic stresses which build up in the initial rapid stages of swelling.

**Acknowledgment.** We thank AstraZeneca (UK) Ltd. for supporting this project as part of their Strategic Research Fund, particularly Jonathan Booth for providing the materials. We also thank Kari Dalnoki-Veress

for useful discussions during the construction of the humidity cell.

### References and Notes

- (1) Thomas, N. L.; Windle, A. H. *Polymer* **1982**, *23*, 529–542.
- (2) Jain, R.; Shah, N. H.; Malick, A. W.; Rhodes, C. T. *Drug Dev. Ind. Pharm.* **1998**, *24*, 703–727.
- (3) Heller, J. *Adv. Drug Delivery Rev.* **1993**, *10*, 163–204.
- (4) Wise, D. L.; Fellmann, T. D.; Sanderson, J. E.; Wentworth, R. L. *Drug Carriers in Biology and Medicine*; Academic Press: New York, 1979.
- (5) Lewis, D. H. *Biodegradable Polymers as Drug Delivery Systems*; Marcel Dekker: New York, 1980.
- (6) Mason, W. P. *Physical Acoustics: Principles and Methods*; Academic Press: New York, 1964; p 367. The reader is referred to this text for a diagram illustrating the principal cuts for quartz crystals.
- (7) Li, S.; McCarthy, S. *Biomaterials* **1999**, *20*, 35–44.
- (8) Sauerbrey, G. *Ž. Phys.* **1959**, *155*, 206.
- (9) Rodahl, M.; Höök, F.; Krozer, A.; Brzezinski, P.; Kasemo, B. *Rev. Sci. Instrum.* **1995**, *66*, 3924.
- (10) Rodahl, M.; Höök, F.; Fredriksson, C.; Keller, C. A.; Krozer, A.; et al. In *Faraday Discussions: Interactions of Acoustic Waves with Thin Films and Interfaces*; Royal Society of Chemistry: London, 1997; pp 229–246.
- (11) Chen, W.; Shull, K. R.; Papatheodorou, T.; Styrkas, D. A.; Keddie, J. L. *Macromolecules* **1999**, *32*, 136–144.
- (12) Jones, R. A. L.; Richards, R. W. *Polymers at Surfaces and Interfaces*; Cambridge University Press: New York, 1999.
- (13) Ferry, J. D. *Viscoelastic Properties of Polymers*, 3rd ed.; Wiley: New York, 1980.
- (14) Forrest, J. A.; Dalnoki Veress, K. *Adv. Colloid Interface Sci.*, in press.
- (15) Lide, D. R., Ed.; *CRC Handbook of Chemistry and Physics*; CRC Press: London, 1998–1999.
- (16) Hui, C. Y.; Wu, K. C.; Lasky, R. C.; Kramer, E. J. *J. Appl. Phys.* **1987**, *61*, 5129.
- (17) Brandrup, J.; Immergut, E. H. *Polymer Handbook*, 3rd ed.; Wiley: New York, 1989.
- (18) Rodahl, M. *Sens. Actuators, A* **1996**, *54*, 448–456.

MA011163Q